

# Comparison between the Linked Color and White Light Imaging Combined Score in the Evaluation of High-Risk Population of Gastric Cancer

Jiang Zhang Xiu<sup>1D</sup>, Nong Bing<sup>1D</sup>, Ning Jia Juan<sup>1D</sup>, Huang Peng Yu<sup>1D</sup>

Department of Digestion, The People's Hospital of Guangxi Zhuang Autonomous Region, Nanning, P. R. China

**Cite this article as:** Xiu JZ, Bing N, Juan NJ, Yu HP. Comparison between the linked color and white light imaging combined score in the evaluation of high-risk population of gastric cancer. *Turk J Gastroenterol.* 2021; 32(10): 859-869.

## ABSTRACT

**Background:** For patients undergoing gastroscopy, it is necessary to judge whether there is *Helicobacter pylori* infection, atrophy/intestinal metaplasia. This study aimed to evaluate and compare the light color imaging (LCI) and white light imaging (WLI) combined score during gastroscopy.

**Methods:** Each included patient underwent normalized gastroscopy with WLI and LCI, and all notable findings were photographed. Four endoscopists reviewed the endoscopic images of each patient. The clinical information, results of the *H. pylori* tests were unavailable at review. The total LCI and WLI scores of each patient were calculated and their detection in high-risk populations of gastric cancer were evaluated. The diagnostic values of LCI and WLI for intestinal metaplasia were also calculated.

**Results:** In total, 392 patients were included in the study. The degree of inflammation and proportion of active inflammation cases were significantly higher in the *H. pylori* gastritis group than in the non-*H. pylori* gastritis group; their endoscopic manifestations were also different. The LCI combined score improved the diagnostic value of each individual observation index in the diagnosis of *H. pylori* infection compared with the WLI combined score. The sensitivity, specificity, and accuracy were 91.9% (91.9% vs 81.5%), 91.1% (91.1% vs 80.2%), and 95.8% (95.8% vs 93.2%), respectively. The accuracy of LCI in the diagnosis of intestinal metaplasia was higher than that of WLI (83.4% vs 69.6%).

**Conclusion:** The LCI and LCI combined score improved the diagnosis of *H. pylori* gastritis and intestinal metaplasia, and it is considered valuable in identifying the high-risk population of gastric cancer.

**Keywords:** Linked color imaging, white light imaging, endoscopy, combined score, *Helicobacter pylori* gastritis, intestinal metaplasia

## INTRODUCTION

Approximately 89% of gastric cancer cases are associated with *Helicobacter pylori* gastritis.<sup>1,2</sup> The eradication of *H. pylori* before the occurrence of irreversible injury to the gastric mucosa is effective in preventing gastric cancer.<sup>3</sup> Thus, early diagnosis of *H. pylori* gastritis is essential in inhibiting disease progression.

The diagnosis of *H. pylori* infection is essential for patients undergoing endoscopy because of upper gastrointestinal symptoms and other factors. Currently, the available endoscopic methods for the diagnosis of *H. pylori* infection include standard white light endoscopy, magnifying endoscopy combined with narrow-band imaging (NBI), and staining endoscopy.<sup>4,5</sup> However, the accuracy and consistency of these methods in assessing the indicators of infection are low.<sup>5</sup> Magnifying endoscopy combined with NBI or staining has a higher accuracy than that of

traditional endoscopy in the diagnosis of *H. pylori* gastritis; however, the need for observers, equipment, and time is higher. The results of different studies on endoscopic diagnosis of atrophic/intestinal metaplasia were quite different.<sup>6-10</sup>

Light color imaging (LCI) is a newly developed endoscopic technique, characterized by sensitivity to color differentiation, that can detect slight changes in color associated with pathological changes in the mucosa of the digestive tract. Recent studies have shown that LCI has a higher accuracy in diagnosing *H. pylori* gastritis than of white light imaging (WLI).<sup>11,12</sup> In relation to this, our previous study has indicated that LCI is more sensitive, specific, and accurate in diagnosing *H. pylori* gastritis than is traditional endoscopy. Despite these findings, the accuracy of each individual index of LCI remains low. Whether the diagnostic accuracy can

Corresponding author: Nong Bing, e-mail: j272162290@163.com

Received: September 17, 2020 Accepted: February 22, 2021 Available Online Date: November 1, 2021

© Copyright 2021 by The Turkish Society of Gastroenterology · Available online at [turkjgastroenterol.org](http://turkjgastroenterol.org)

DOI: 10.5152/tjg.2021.20799

increase significantly if the indices are combined was unclear.

## MATERIALS AND METHODS

### Patients

A prospective comparative interventional study was conducted. Patients who underwent gastroscopic examination at our hospital because of upper gastrointestinal symptoms, suspected upper gastrointestinal lesions or atrophic gastritis, gastric ulcer, and precancerous lesions of gastric cancer between November 2019 and May 2020 were included. The exclusion criteria were as follows: (a) patients younger than 18 years; (b) those who were not suitable candidates for endoscopic biopsy; (c) those who had undergone gastrectomy; (d) those who had been taking proton pump inhibitors, antibiotics, or non-steroidal anti-inflammatory drugs within 2 weeks before the procedure; and (e) those with cirrhotic portal hypertension or other conditions that may affect the diagnosis of *H. pylori* gastritis. All patients provided written informed consent for endoscopy, and the study was approved by the ethics committee of our institution.

### Endoscopy

All examinations were performed with a high-definition EGL590WR endoscope similar to the LASEREO endoscopic system (Fujifilm, Tokyo, Japan). This system has white light mode, BLI-bright mode, and LCI mode. The wavelength of the white light mode observation laser is  $450 \pm 10$  nm. The principle is to let the fluorescent body emit high-efficiency light and to mix the high-efficiency light with the fluorescent body as white light. Through the fluorescent body, wide spectrum and high-brightness white light suitable for routine inspection can be emitted; Thus, the natural color image can be observed on the monitor. The BLI-bright observation laser ( $410 \pm 10$  nm) is a narrow-band light that can emphasize surface treatment, and it is irradiated after

mixing with white light. Because of its short light wave and narrow spectrum, it can be used for morphological observation of the lesions by highlighting the contrast of the microvessels and micro-convexity of the mucosal surface to achieve narrow-band light observation while maintaining brightness. The LCI mode is based on the illumination ratio of the BLI-bright 2-beam laser; the image obtained is processed using a host software. In this mode, the image captured is subjected to further post-image processing that makes a slightly reddish color more red, and a slightly whitish color more white compared with the colors in WLI.<sup>2,13</sup>

### Examination Protocol

Two experienced endoscopists performed all examinations. The patients were classified into the LCI-WLI group and the WLI-LCI group via simple randomization. Patients in the LCI-WLI group were first assessed in the LCI mode. Then, another examiner who was unaware of the results of the previous examination evaluated the patient in the WLI mode. Patients in the WLI-LCI group were first assessed in the WLI mode and then in the LCI mode.

During endoscopy, all images were obtained in the following order: (a) mucus lake (antegrade view first), (b) gastric body wall (greater curvature and posterior view), (c) gastric antrum walls (then retroflex view), (d) gastric angle (retroflex view), (f) gastric body (small curved side), (g) fundus, and (h) gastric body walls (antegrade view last).

### Biopsy Protocol

After completing the standard endoscopy, biopsy was performed in the antrum and body of the stomach. The rapid urease test was performed to assess 2 separate biopsy specimens from the antrum and corpus. The specimens for pathological examination were fixed in 10% formalin and embedded in paraffin. The sections were then stained with hematoxylin and eosin, Giemsa, Alcian blue, and Periodic acid-Schiff for histopathologic examination. Assessment of *H. pylori* gastritis, atrophy, and intestinal metaplasia was performed according to the updated Sydney System.<sup>14,15</sup>

### Analysis of Endoscopic Images

The endoscopic images were evaluated by 4 endoscopists who did not perform the procedure and were blinded to the clinical data. Two of the expert endoscopists have performed >10 000 conventional endoscopy procedures, whereas the 2 non-expert endoscopists have performed <500 conventional endoscopy procedures.

## MAIN POINTS

- The degree of inflammation and proportion of active inflammation cases were significantly higher in the *H. pylori* gastritis group than in the non-*H. pylori* gastritis group; their endoscopic manifestations were also different.
- The light color imaging (LCI) and LCI combined score improved the diagnosis of *H. pylori* gastritis and intestinal metaplasia.
- The LCI and LCI combined scores were considered valuable in identifying the high-risk population of gastric cancer.

The endoscopists were trained in LCI by a certified endoscopic specialist. The training involved comparison of colors from 100 endoscopic images and an international standard chromogram to identify microstructures and colors on the mucosal surface. This process was considered complete when the endoscopists could consistently and accurately identify the color of the mucosa, mucous lake, and microstructure.

The endoscopic observation indices of WLI included erythema, map-like redness, flat villous eminence, erosions (superficial defects <5 mm in the mucosa with a flat edge), nodularity (fine or coarse nodular deformity of the normal smooth mucosal lining on tangential view), and regular arrangement of collecting venules (RAC).<sup>5,12,13</sup> Our preliminary experiment revealed that the following observation indices were associated with *H. pylori* infection in the LCI mode compared with the international standard chromogram: redness of the

fundic gland mucosa (color of the fundus gland close to 710-711C or 1788 2XC of the international standard chromogram), purple mucus (+) (color of the surface of the gastric mucosa close to 674-675C of the international standard chromogram), coexistence of redness of the fundic gland mucosa and purple mucus (with a color between 710 and 711C and 674-675C), muddy lake turbidity (color of the mucous lake close to 663C-665C and 5875C of the international standard chromogram; contained uniform white particles), and granular erosion (granular surface microstructure, covered with mucus and granular white opacity). At the same time, we defined lavender purple positive as patchy or map-like mucosa color close to 673-674C<sup>5,16</sup> (Figure 1). Thus, endoscopic examination in the LCI mode included all previously described indicators.

First, 4 doctors blinded to the diagnostic results evaluated the images, and the consistency of diagnosis

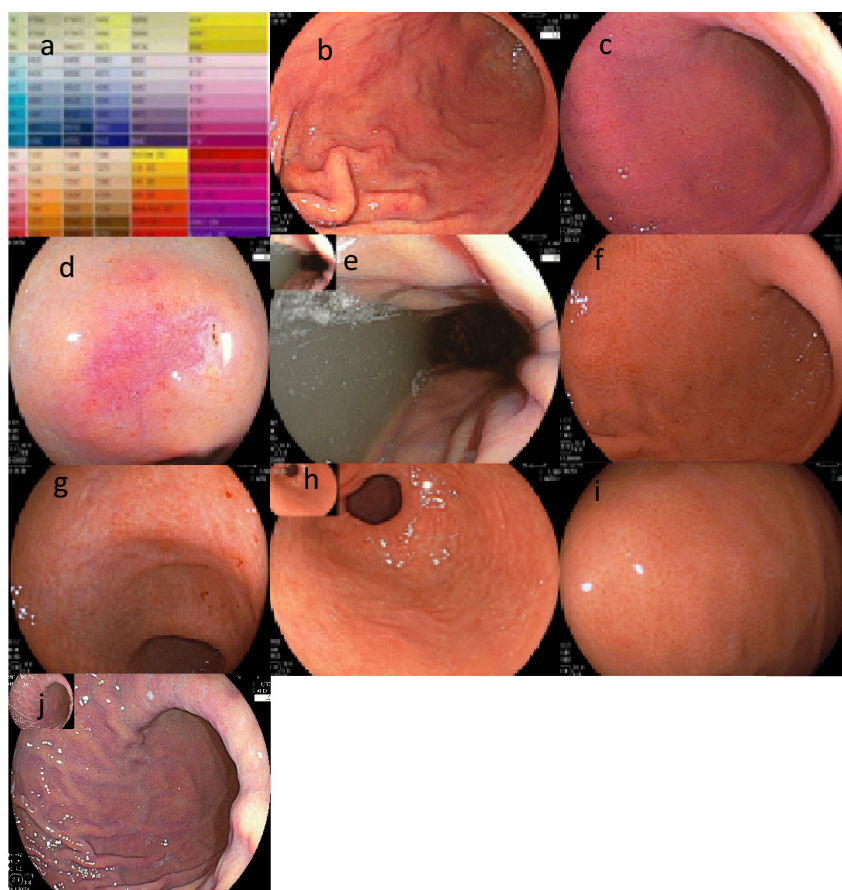


**Figure 1.** (A) International standard chromogram, (B) Fundic gland mucosa redness, (C) Fundic gland mucosa redness and purple mucus coexist, (D) Granular erosion, (E) Muddy lake turbidity, (F) Erythema, invisible regular arrangement of collecting venules (RAC), (G) Erosions, (H) Nodularity, (I) Normal mucosa, visible RAC, (J) Purple mucus.

between expert/non-expert endoscopists was evaluated. Then, the expert/non-expert endoscopists discussed the results that were inconsistent and reached an agreement, and the sensitivity, specificity, and accuracy of diagnosis in the 2 groups were evaluated.

### Diagnosis of *H. pylori* Infection

All patients were classified under the *H. pylori* gastritis or the non-*H. pylori* gastritis groups on the basis of the results of pathological examination, the carbon-14 urea breath test, and positive urease test findings<sup>6</sup> (Figure 2). According to pathology, they were divided into atrophic/intestinal metaplasia subgroup.

### Statistical Analysis

A correlation analysis was performed to evaluate the relationship between each individual observation index of LCI (i.e., redness of fundic gland mucosa, purple mucus (+), mucous lake turbidity, and granular erosion) and *H. pylori* infection. Moreover, the correlation between each individual observation index of WLI (erythema, presence of erosions, nodularity, and invisible RAC) and *H. pylori* gastritis was assessed. A logistic regression analysis of the 2 classification variables was subsequently conducted to examine the observation indices that were useful for the differential diagnosis of *H. pylori* gastritis. The corresponding partial regression coefficients were then calculated. As each observation unit is consistent, the partial regression coefficient represents the contribution of each individual observation index; thus, different observation indices were scored according to the partial regression coefficients. This system was used to score WLI and LCI by calculating the total scores of all patients. Finally, a correlation analysis was used to evaluate the relationship between the total scores and *H. pylori* gastritis. The

receiver operating characteristic (ROC) curve was used to determine the differential diagnosis of gastritis due to *H. pylori* infection or another variable. The corresponding sensitivity, specificity, and area under the curve were calculated for the ROC curve. Interobserver agreement was quantified using the kappa statistic. Kappa values (coefficient of consistency) <0.20, 0.21-0.40, 0.41-0.60, 0.61-0.80, and >0.80 indicated poor, fair, moderate, good, and excellent agreement, respectively. A *P*-value <.05 was considered statistically significant. All statistical analyses were performed using the Statistical Package for the Social Sciences software version 22.0. The chi-square test was used to compare the different assessment methods.

### RESULTS

In total, 392 patients were included in the study. The mean age of the participants was  $50.8 \pm 13.4$  (range: 18-79) years. Moreover, 155 (39.5%) patients were men and 237 (60.5%), women. Furthermore, 135 (34.2%) patients were included in the *H. pylori* gastritis group and the remaining 257 (65.8%), in the *H. pylori*-negative group. No significant difference was observed in terms of age and sex between the 2 groups (Table 1; *P* > .05). There were 116 cases (87.9%) of moderate-severe inflammation and 16 cases of mild inflammation in the *H. pylori* gastritis group and 74 cases (28.9%) of moderate-severe inflammation in the non-*H. pylori* gastritis group, indicating a significant difference between the groups, *P* < .01. In the *H. pylori* gastritis group, 47.6% of the patients with and 17.3% without lymphofollicular hyperplasia showed sheet redness of the mucosa indicating a significant difference; the rest of the patients showed diffuse redness of the mucosa.

The correlation coefficients of each individual observation index and *H. pylori* gastritis are shown in Table 2. For expert

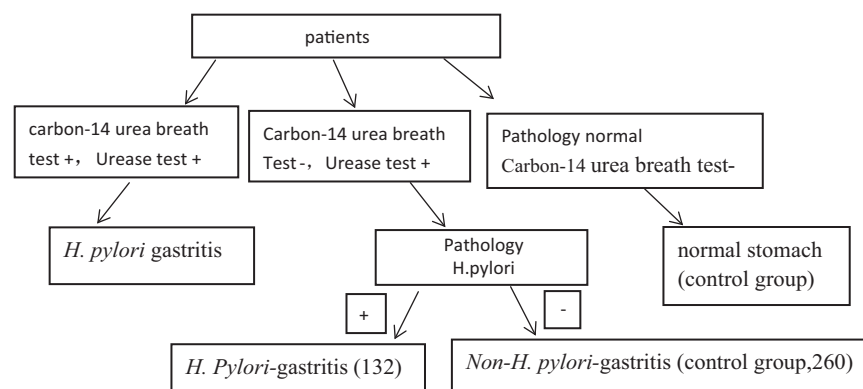


Figure 2. Determination of *Helicobacter pylori* gastritis group and control group.

**Table 1.** Characteristics of the Total 392 Study Subjects

Factor	Total 392 Study Subjects	<i>Helicobacter pylori</i> Infection (+)	<i>Helicobacter pylori</i> Infection (–)
Age (years)	50.8 ± 13.4	60.3 ± 27.8	57.7 ± 24.3
Range	18-78	18-78	19-75
Sex			
Male	155	54	101
Female	237	78	159
Intestinal metaplasia	161	56	105
Active inflammation	156	132	24
Experts			
Redness of the fundus gland mucosa	146	115	31
Mucous lake turbidity	184	112	72
Purple mucus	139	102	37
Granular erosion	31	29	2
Erythema	165	103	62
Invisible RAC	177	94	83
Visible RAC	216	40	176
Lavender purple	164	130	34
Map-like redness and white villous eminence	182	112	70
Non-Experts			
Redness of the fundus gland mucosa	170	112	58
Mucous lake turbidity	146	69	77
Purple mucus	132	78	54
Granular erosion	51	37	14
Erythema	159	96	63
Invisible RAC	166	79	87
Visible RAC	240	79	161
Lavender purple	175	115	60
Map-like redness and white villous eminence	165	99	66

endoscopists, correlation analysis revealed that purple mucus (+), mucus lake turbidity, redness of the fundic gland mucosa, and LCI scores were significantly correlated to *H. pylori* infection, and their correlation coefficients were 0.618, 0.611, 0.730, and 0.762, respectively ( $P < .05$ ). A low-to-moderate correlation was observed between loss of collecting venules (invisible RAC), erythema, and *H. pylori* infection. Moreover, their correlation coefficients were 0.366 and 0.488, respectively ( $P < .05$ ). Map-like redness/white villous eminence and lavender purple were moderately associated with intestinal metaplasia. For non-expert endoscopists, redness of the fundic gland mucosa

and LCI scores were moderately associated with *H. pylori* infection, and their correlation coefficients were 0.463–0.496 ( $P < .05$ ). The other observational indices were moderately correlated to *H. pylori* gastritis. Meanwhile, erosions and nodularity were not associated with *H. pylori* infection. Map-like redness/white villous eminence and lavender purple were moderately associated with intestinal metaplasia.

The logistic regression model analysis revealed that the observation indices (redness of the fundic gland mucosa, granular erosion, purple mucus (+), and mucus lake turbidity) had significant fitting curves and were useful for



**Table 2.** Correlation Coefficients of Individual Observation, Scores of 2 Modes and *H. pylori* Gastritis

Observers	Correlation Coefficient	P
<b>Experts</b>		
Redness of the fundus gland mucosa	0.730	.000
Mucous lake turbidity	0.611	.000
Purple mucus (+)	0.618	.000
Granular erosion	0.469	.000
Erythema	0.488	.000
Erosion	0.470	.165
Nodularity	−0.415	.765
Invisible RAC	0.466	.000
WLI scores	0.702	.000
LCI scores	0.762	.000
Lavender violet	0.701	.000
Map-like redness and white villous eminence	0.603	.000
<b>Non-Experts</b>		
Redness of the fundus gland mucosa	0.563	.000
Mucous lake turbidity	0.430	.000
Purple mucus (+)	0.494	.000
Granular erosion	0.450	.003
Erythema	0.416	.000
Erosion	0.314	.025
Nodularity	0.037	.464
Invisible RAC	−0.379	.000
WLI scores	0.508	.000
LCI scores	0.506	.000
Lavender violet	0.654	.000
Map-like redness and white villous eminence	0.451	.000

LCI, light color imaging; WLI, white light imaging; RAC, regular arrangement of collecting venules.

the diagnosis of *H. pylori* gastritis. For the expert endoscopists, the partial regression coefficients of these indexes were 2.979, 3.613, 1.308, and 1.389, respectively. Each individual observation index was scored according to the approximate value of the partial regression coefficient. Redness of the fundic gland mucosa was scored with 3 points; granular erosion, 3.5 points; and purple mucosa and mucus lake turbidity, 1 point. In the WLI mode, the loss of collecting venules (1.174) and erythema (1.203) had significant fitting curves. Their partial regression coefficients were similar, each with a score of 2. The endoscopic images of these 2 modes were scored according to these criteria, and the total scores were calculated.

The sensitivity, specificity, accuracy, positive predictive value, and negative predictive value of the LCI combined scores obtained by the expert endoscopists were 91.9%, 91.1%, 95.8%, 85.4%, and 95.5%, respectively. Each individual observation and the total scores for the differential diagnosis of gastritis due to *H. pylori* or other variables are depicted in Table 3. The diagnostic accuracy of the LCI and WLI scores was higher than that of each individual observation index of each mode ( $P < .05$ ).

The value of lavender purple in diagnosis of intestinal metaplasia was higher than that of map-like red/white villous protuberance (Table 4).

**Table 3.** The Sensitivity and Specificity of Total Scores and Each Observation Index in the Diagnosis of *Helicobacter pylori* Gastritis

	Sensitivity (%)	Specificity (%)	Area Under Curve (%)	Positive Predictive Value (%)	Negative Predictive Value (%)
<b>Experts</b>					
Redness of the fundus gland mucosa	86.5	88.0	87.2	78.8	93.1
Mucous lake turbidity	84.2	72.1	78.2	60.9	90.4
Purple mucus (+)	76.7	85.9	81.4	73.4	88.1
Granular erosion	21.8	99.2	60.5	93.5	71.5
LCI scores $\geq 2.75$	91.9	91.1	95.8	85.4	95.5
Erythema	76.7	76.1	76.4	64.0	87.4
Invisible RAC	70.7	67.8	69.3	53.1	82.3
WLI scores $>1.5$	81.5	80.2	83.2	67.8	89.2
<b>Non-Experts</b>					
Redness of the fundus gland mucosa	82.7	77.6	79.2	64.3	90.2
Mucous lake turbidity	52.3	70.0	61.1	47.3	74.4
Purple mucus (+)	59.1	79.3	69.2	59.1	66.3
Granular erosion	28.0	94.5	61.3	72.5	72.1
LCI score $\geq 2.75$	84.2	81.5	82.8	69.9	91.9
Erythema	71.4	75.7	73.6	62.2	82.6
Invisible RAC	59.8	66.0	62.9	47.6	76.5
WLI scores $>1.5$	82.7	74.1	80.7	60.0	90.2

LCI, light color imaging; WLI, white light imaging; RAC, regular arrangement of collecting venules.

The coefficients of consistency between expert/non-expert endoscopists are shown in Table 5. For expert endoscopists, the consistency for each individual observation index was good-excellent in the LCI mode (0.631-0.801). In the WLI mode, the consistency between expert

endoscopists for erythema and invisible RAC, which are both significant indicators in the diagnosis of *H. pylori* gastritis, was good. The consistency between non-expert and expert endoscopists for all observation indices was moderate.

**Table 4.** The Sensitivity and Specificity of White Light Imaging and Light Color Imaging in the Diagnosis of Intestinal Metaplasia

	Sensitivity (%)	Specificity (%)	Area Under Curve (%)	Positive Predictive Value (%)	Negative Predictive Value (%)
<b>Experts</b>					
Map-like redness and white villous eminence	69.6	74.9	69.6	61.5	82.4
Lavender purple (+)	80.7	85.3	83.4	79.3	86.4
<b>Non-Experts</b>					
Map-like redness and white villous eminence	61.5	71.5	67.3	60.0	72.7
Lavender purple (+)	71.4	74.0	79.2	65.7	78.8

**Table 5.** Kappa Values (Coefficient of Consistency) Between Experts and Non-experts

Observer	Kappa Values	P
<b>Between Experts</b>		
Redness of the fundus gland mucosa	0.732	.000
Mucous lake turbidity	0.611	.000
Purple mucus (+)	0.613	.000
Granular erosion	0.767	.000
Erythema	0.631	.000
Invisible RAC	0.648	.000
Map-like redness and white villous eminence	0.735	.000
Lavender purple (+)	0.801	.000
LCI scores	0.621	.000
WLI scores	0.590	.000
<b>Between Non-Experts</b>		
Redness of the fundus gland mucosa	0.620	.000
Mucous lake turbidity	0.518	.000
Purple mucus (+)	0.524	.000
Granular erosion	0.598	.000
Erythema	0.630	.000
Invisible RAC	0.599	.036
Map-like redness and white villous eminence	0.654	.000
Lavender purple(+)	0.700	.000
LCI scores	0.542	.000
WLI scores	0.400	.000
<b>Experts and Non-Experts</b>		
Redness of the fundus gland mucosa	0.600	.000
Mucous lake turbidity	0.409	.000
Purple mucus(+)	0.532	.000
Granular erosion	0.459	.000
Erythema	0.539	.000
Invisible RAC	0.550	0.000
Map-like redness and white villous eminence	0.621	0.000
Lavender purple(+)	0.734	0.000
LCI scores	0.587	0.000
WLI scores	0.506	0.000

LCI, light color imaging; WLI, white light imaging; RAC, regular arrangement of collecting venules.

## DISCUSSION

*Helicobacter pylori* infection is associated with inflammatory injury characterized by neutrophil (acute phase) and eosinophil/monocyte infiltration (chronic phase);<sup>17</sup> atrophy/intestinal metaplasia may occur during the development,

which is correlated with gastric cancer.<sup>2,13,14</sup> These varying phases and levels of inflammation can differentially affect the performance of endoscopy. Data obtained using WLI showed that erythema, erosions, nodularity, ulcer, and fold hyperplasia can exist alone or in combination.



An invisible RAC can be observed if there is inflammation or hyperplasia of the gastric mucosa. A clearly observed RAC may indicate a normal mucosa. These appearances can also be observed in the LCI mode, which is highly sensitive to color differences in the surface microstructure of the mucosa because of factors such as different color of the marginal crypt epithelium, the intervening part, and the crypt opening, and inflamed glandular tube at the edge of erosion. Furthermore, proliferation of the glandular epithelium leads to increased secretion of mucus, which is purple on LCI. The mucus lake is cloudy on endoscopy because of the increased secretion of mucus, which causes the mucosa to have a purple sand-papered appearance. Thus, red mucosa, purple mucus, granular erosion, and mucus lake turbidity were included in the scope of observation.

In this study, we performed a correlation analysis to assess the indicators associated with *H. pylori* infection. The WLI and LCI scores, redness of the fundic gland mucosa, purple mucosa, and mucus lake turbidity were significantly correlated with *H. pylori* infection, on the basis of the results obtained by experienced endoscopists. In contrast, granular erosion, erythema, and loss of collecting venules were moderately correlated with *H. pylori* infection. No significant correlation was observed between residual indicators and *H. pylori* gastritis. Because of the different endoscopic characteristics of *H. pylori* gastritis, the diagnosis of *H. pylori* infection on the basis of a single endoscopic characteristic is considered inaccurate.

The study results showed that the sensitivity, specificity, and accuracy of each individual observation index of WLI for the diagnosis of *H. pylori* gastritis had a moderate interobserver agreement between examiners. Previous studies have reported that the LCI patterns are more sensitive than the WLI patterns in the diagnosis of *H. pylori* infection.<sup>5</sup> However, because of varying endoscopic characteristics, the specificity and accuracy of the redness of the gastric fundus mucosa or other individual endoscopic features for the diagnosis of *H. pylori* infection are not extremely high. Meanwhile, our results showed that all indices had an accuracy <90% for *H. pylori* gastritis. This may be related to different inflammation states and levels. Our study showed that most of the patients who had *H. pylori* gastritis with lymphofollicular hyperplasia and lymphocytic infiltration showed sheet redness of the mucosa on endoscopic findings, which may be related to the fact that lymphofollicular hyperplasia can limit the spread of inflammation. Infiltration of different inflammatory cells results in different endoscopic manifestations.

Therefore, the effectiveness of the observation indices in confirming the diagnosis can be affected if each one is used in isolation. Therefore, logistic regression analysis was performed to further assess the observation indices of *H. pylori* infection in the WLI mode. Then, the WLI combined scores were calculated to improve the diagnostic rate of endoscopy. Our results showed that erythema and invisible RAC, but not erosions and nodularity, were included in the regression model, which was useful for the differential diagnosis of *H. pylori* gastritis. These results are consistent with those obtained by correlation analysis. On the basis of the corresponding partial regression coefficient, each index scored 2 points, and ROC analysis was conducted to evaluate the value of the total scores in the diagnosis of *H. pylori* gastritis. Our findings showed that the sensitivity and specificity were higher than each single observation index if a total score of 1.5 was used as the cut-off value for diagnosis, but the accuracy was still low.

Moreover, logistic regression model analysis was performed to assess the endoscopic indicators that were considered useful for the diagnosis of *H. pylori* gastritis in the LCI mode. Each index was scored according to weight, and the total scores of each patient were calculated. Logistic regression model analysis revealed that redness of the fundic gland mucosa, mucus lake turbidity, purple mucosa (+), and granular erosion had significant fitting curves. According to the scoring criteria, these observation indices play an essential role in the diagnosis of *H. pylori* infection. An obvious synergistic effect was observed among the observation indices. The sensitivity, specificity, and accuracy of the LCI combined score in the diagnosis of *H. pylori* gastritis were 87.2%, 91.1%, and 94.4%, respectively, which were higher than those of the individual indices. Meanwhile, the diagnostic value of the LCI combined score was significantly higher than that of the WLI combined score and each individual observation index of WLI. The effectiveness of the LCI score in the differential diagnosis of *H. pylori* gastritis may be related to the pathological characteristics of the disease. Our study showed that 87.9% of the patients with *H. pylori* gastritis had moderate-severe inflammation, and all of them had active inflammation, while only 28.9% of the patients in non-*H. pylori* gastritis group had moderate-severe inflammation, and only 11.2% of them had active inflammation. Active inflammation of the mucosa results in hyperemia, which is manifested as redness of the mucosa, while mild, inactive inflammation shows no obvious signs on endoscopic examination. LCI is sensitive to the changes in color, so it is a convenient tool for detecting color differences and making a differential diagnosis. Meanwhile,

because infiltration with different inflammatory cells can cause different endoscopic manifestations, the LCI score can enhance the differential diagnosis. For patients with high confidence in the diagnosis of *H. Pylori*-gastritis, there is no need for carbon breath test or pathological detection of *H. Pylori*, which saves the time and cost of treatment.

Atrophic/intestinal metaplasia related to *H. pylori* gastritis is a precancerous state of gastric cancer, and its detection is very important. Serological examination is only sensitive to severe atrophic/intestinal metaplasia, and endoscopy is the main method for the diagnosis of mild atrophic/intestinal metaplasia.<sup>10</sup> The sensitivity, specificity and accuracy of LCI for the diagnosis of intestinal metaplasia were all above 80%, higher than that of WLI.

The consistency test showed that the diagnostic accuracy and consistency of each individual observation index for diagnosis of *H. pylori* gastritis, regardless of mode, among expert endoscopists were significantly higher than those among non-expert endoscopists. The consistency of the LCI or WLI combined score between examiners was lower than that of an individual observation index with high consistency. The combination of individual observation indicators can improve the accuracy of diagnosis. However, to some extent, it reduces the consistency between examiners. To improve diagnostic accuracy and help meet the clinical requirements for consistency between examiners, the consistency of individual observation indices must be improved and subjectivity should be reduced. If more stringent definitions of each observation index can be established, then the occurrence of these issues may be reduced among training physicians who assess imaging results. The consistency among the examiners for the diagnosis of intestinal metaplasia was good, especially in LCI mode.

In summary, different degrees of inflammation, presence/absence of inflammatory activity, and infiltration with different types of inflammatory cells all lead to different manifestations of gastritis on endoscopic findings. LCI had a better resolution of color differences and a higher diagnostic rate of *H. pylori* infection than that of WLI endoscopy. In addition, the LCI combined score synthesized the characteristics of *H. pylori* infection, and its use improved the diagnostic rate of *H. pylori* gastritis. Because this method can predict the presence of *H. pylori* infection, it has an important clinical value in the detection of high-risk patients.

**Ethics Committee Approval:** This study was approved by the Ethics Committee of People's Hospital of Guangxi Zhuang Autonomous Region. The committee's reference number is 2019-002.

**Informed Consent:** All patients provided written informed consent to undergo gastroendoscopy.

**Peer-review:** Externally peer-reviewed.

**Author Contributions:** Project Design – Z.X.J., B.N.; Manuscript Writing – Z.X.J.; Data Collection – J.J.N., P.Y.H.

**Acknowledgments:** We would like to thank all the staff who supported our research.

**Conflict of Interest:** The authors have declared that no conflicts of interest exist.

**Financial Disclosure:** The Guangxi Clinical Medical Research Center for Digestive Diseases (no. AD17129027) provided equipment support for this study.

## REFERENCES

1. Plummer M, Franceschi S, Vignat J, Forman D, de Martel C. Global burden of gastric cancer attributable to *Helicobacter pylori*. *Int J Cancer*. 2015;136(2):487-490. [\[CrossRef\]](#)
2. Fock KM. Review article: The epidemiology and prevention of gastric cancer. *Aliment Pharmacol Ther*. 2014;40(3):250-260. [\[CrossRef\]](#)
3. Sugano K, Tack J, Kuipers EJ, et al. Kyoto global consensus report on *Helicobacter pylori* gastritis. *Gut*. 2015;64(9):1353-1367. [\[CrossRef\]](#)
4. Yagi K, Saka A, Nozawa Y, Nakamura A. Prediction of *Helicobacter pylori* status by conventional endoscopy, narrow-band imaging magnifying endoscopy in stomach after endoscopic resection of gastric cancer. *Helicobacter*. 2014;19(2):111-115. [\[CrossRef\]](#)
5. Gonen C, Simsek I, Sarioglu S, Akpinar H. Comparison of high resolution magnifying endoscopy and standard videoendoscopy for the diagnosis of *Helicobacter pylori* gastritis in routine clinical practice: A prospective study. *Helicobacter*. 2009;14(1):12-21. [\[CrossRef\]](#)
6. Trieu JA, Bilal M, Saraireh H, Wang AY. Update on the diagnosis and management of gastric intestinal metaplasia in the USA. *Dig Dis Sci*. 2019;64(5):1079-1088. [\[CrossRef\]](#)
7. Savarino E, Corbo M, Dulbecco P, et al. Narrow-band imaging with magnifying endoscopy is accurate for detecting gastric intestinal metaplasia. *World J Gastroenterol*. 2013;19(17):2668-2675. [\[CrossRef\]](#)
8. Buxbaum JL, Hormozdi D, Dinis-Ribeiro M, et al. Narrow-band imaging versus white light versus mapping biopsy for gastric intestinal metaplasia: A prospective blinded trial. *Gastrointest Endosc*. 2017;86(5):857-865. [\[CrossRef\]](#)
9. Chen H, Wang H, Wu X, et al. Predictability of gastric intestinal metaplasia by patchy lavender color seen on linked color imaging endoscopy. *Lasers Med Sci*. 2019;34(9):1791-1797. [\[CrossRef\]](#)
10. Ono S, Kato M, Tsuda M, et al. Lavender color in linked color imaging enables noninvasive detection of gastric intestinal metaplasia. *Digestion*. 2018;98(4):222-230. [\[CrossRef\]](#)
11. He Q, Li G, Wang X, et al. A decrease of histone deacetylase 6 expression caused by *Helicobacter pylori* infection is associated with

Q2

oncogenic transformation in gastric cancer. *Cell Physiol Biochem*. 2017;42(4):1326-1335. [\[CrossRef\]](#)

12. Takeda T, Asaoka D, Nojiri S, et al. Linked color imaging and the Kyoto classification of gastritis: Evaluation of visibility and inter-rater reliability. *Digestion*. 2020;101(5):598-607. [\[CrossRef\]](#)

13. Yoshida N, Naito Y, Yasuda R, et al. Linked color imaging improves the visibility of various featured colorectal polyps in an endoscopist's visibility and color difference value. *Int J Colorectal Dis*. 2017;32(9):1253-1260. [\[CrossRef\]](#)

14. Dixon MF, Genta RM, Yardley JH, Correa P. Classification and grading of gastritis. The updated Sydney system. *International*

*Workshop on the Histopathology of Gastritis, Houston 1994*. *Am J Surg Pathol*. 1996;20(10):1161-1181. [\[CrossRef\]](#)

15. Stolte M, Meining A. The updated Sydney system: Classification and grading of gastritis as the basis of diagnosis and treatment. *Can J Gastroenterol*. 2001;15(9):591-598. [\[CrossRef\]](#)

16. Jiang ZX, Nong B, Liang LX, Yan YD, Zhang G. Differential diagnosis of *Helicobacter pylori*-associated gastritis with the linked-color imaging score. *Dig Liver Dis*. 2019;51(12):1665-1670. [\[CrossRef\]](#)

17. Laine L, Cohen H, Sloane R, Marin-Sorensen M, Weinstein WM. Interobserver agreement and predictive value of endoscopic findings for *H. pylori* and gastritis in normal volunteers. *Gastrointest Endosc*. 1995;42(5):420-423. [\[CrossRef\]](#)

**Author Queries**

JOB NUMBER: 20200799

JOURNAL: TJG

Q1 Please check the usage of LCI in this sentence.

Q2 The Reference no. 6 is a duplicate of Reference no. 5. The Reference no. 15 is a duplicate of Reference no. 2. The Reference no. 16 is a duplicate of Reference no. 14. The Reference no. 19 is a duplicate of Reference no. 5. The Reference no. 22 is a duplicate of Reference no. 11. Please check and confirm.